



## Data Article

# Geochemical and magnetic data on anthropogenic ashes from municipal solid waste incineration (MSWI)



Valerio Funari<sup>a,\*</sup>, Luciana Mantovani<sup>b</sup>, Luigi Vigliotti<sup>a</sup>,  
Enrico Dinelli<sup>c</sup>, Mario Tribaudino<sup>b</sup>

<sup>a</sup> Dipartimento di Scienze del Sistema Terra e Tecnologie per l'Ambiente, Consiglio Nazionale delle Ricerche, ISMAR-CNR Bologna Research Area, Bologna, Italy

<sup>b</sup> Dipartimento di Scienze Chimiche, della Vita e della Sostenibilità Ambientale, Università degli Studi di Parma, Parma, Italy

<sup>c</sup> Dipartimento di Scienze Biologiche Geologiche e Ambientali, Alma Mater Studiorum - Università di Bologna, Bologna, Italy

## ARTICLE INFO

## Article history:

Received 21 April 2020

Revised 12 May 2020

Accepted 13 May 2020

Available online 21 May 2020

## Keywords:

Municipal Solid Waste Incineration (MSWI)  
fly ashes

Municipal Solid Waste Incineration (MSWI)  
bottom ashes

X-ray fluorescence (XRF)

Magnetic properties

Magnetic hysteresis

Waste management

Urban mining

## ABSTRACT

This paper reports supplementary information to “Understanding room-temperature magnetic properties of anthropogenic ashes from municipal solid waste incineration to assess potential impacts and resources” [1]. The sample-set is composed of 47 samples of bottom (BA) and fly (FA) ashes from Municipal Solid Waste Incineration (MSWI), including eight magnetic extracts of selected BA and FA materials. The sampling relies on a simple random sampling strategy at four different MSWI sites in Northern Italy [2]. X-Ray Fluorescence (XRF) analysis on pressed powder pellets, microscopic observations on thin sections and stubs, and magnetic analysis were carried out.

Various magnetic measurements are presented: the magnetic susceptibility measured at two different frequencies (0.47 and 4.7 kHz); the mass-specific susceptibility of ARM ( $\chi_{ARM}$ ), expressed in  $\text{m}^3/\text{kg}$ , calculated after mass-normalization and bias DC field correction; experiments for isothermal remanent magnetization (IRM) experimented were also conducted. The latter measurement allowed the calculation of additional parameters, such as the coercivity of remanence

\* Corresponding author.

E-mail address: [valerio.funari@bo.ismar.cnr.it](mailto:valerio.funari@bo.ismar.cnr.it) (V. Funari).

( $B_{0cr}$ ) and the S-ratio [3]. The IRM acquired in a field of 1.0 T was regarded as the saturation IRM (SIRM). Mass-specific magnetic susceptibility ( $\chi$ ) was calculated by dividing the volume susceptibility by the sample mass. Finally, hysteresis loops and backfield curves at room temperature were measured on selected samples and are available. Data can be reused as groundwork information in future studies on MSWI residues. It would be essential to produce new data on geochemical and magnetic characteristics of MSWI residues to assure good coverage of data for enhanced sustainability of these heterogeneous streams of anthropogenic materials. This combination of methods will contribute to paving the way for quick and reliable resource assessment as well as to promote environmental sustainability.

© 2020 The Authors. Published by Elsevier Inc.

This is an open access article under the CC BY-NC-ND license. (<http://creativecommons.org/licenses/by-nc-nd/4.0/>)

Specifications Table

Subject	Environmental Sciences
Specific subject area	Waste management and disposal, resource recycling, geochemistry, environmental rock magnetism
Type of data	Table Image Graph Figure
How data were acquired	Microscope, SEM, XRD, magnetometer, magnetic susceptibility meter, XRF, IRM software, R 3.6.0, R package GCDKit, Microsoft Excel, Minitab
Data format	Raw Analyzed Filtered
Parameters for data collection	Dried, homogenized samples, ensuring samples' representativeness, data quality assured using standard reference materials and procedures.
Description of data collection	Data were collected according to the standard procedure for XRF analysis [2] for magnetic analysis [4, 5, 6], and for statistical data analysis [7]
Data source location	Institution: Department BiGEA, ISMAR-CNR City/Town/Region: Bologna, Emilia-Romagna Country: Italy
Data accessibility	With the article.
Related research article	Author's name Funari V., Mantovani L., Vigliotti L., Dinelli E., Tribaudino M. Title <b>Understanding room-temperature magnetic properties of anthropogenic ashes from municipal solid waste incineration to assess potential impacts and resources</b> Journal <b>Journal of Cleaner Production</b> DOI <a href="https://doi.org/10.1016/j.jclepro.2020.121209">https://doi.org/10.1016/j.jclepro.2020.121209</a>

Value of the Data

- Data are comprehensive information about combined magnetic and geochemical analyses for MSWI residues. They are helpful for adequate comparison with other similar data paving the way for resource recycling from MSWI residues and the assessment of their environmental impacts.
- These data can provide a ground basis for new multidisciplinary works on MSWI residues. The scientific community (geochemists, magnetists, engineers), waste managers, public authorities and stakeholders, decision-makers can use the suggested combination of methods as a tool in waste management for rapid assessment of environmental impacts and resources prospection.

- The data presented here can be compared with new magnetic and geochemical data from MSWI facilities. They can also serve as complementary information for other experiments (e.g., LCA, experiments of magnetic separation, resource recycling from MSWI residues). When good coverage of data becomes available, data integration using the suggested tool is critical for a comprehensive assessment of heterogeneous waste flows such as MSWI residues.
- These room-temperature magnetic data are relatively fast and cheap to measure; XRF analysis is one of the most robust geochemical data, which were additionally checked for quality via international round-robin tests. Their integration is found to be adequate to identify mineral resources and environmental criticalities quickly. In addition, good transferability of the methodology can be surmised to other waste types.

## 1. Data Description

The data presented here detail the observation and findings that are mentioned in the companion article [1] as supportive tables and figures prefixed with an S. The sample materials are Municipal Solid Waste Incineration (MSWI) fly ash (FA) and bottom ash (BA).

### S1. DATA on magnetic properties of the sample materials

A brief overview of typical rock magnetic parameters and their meaning is reported in the supplementary materials (Table S1). Figure S1 represents hysteresis loops at room temperature (raw data) for a BA sample and the corresponding (more) diamagnetic fraction extracted using a Frantz magnetic separator (see [1] for further details). Data plotted on the “Day” plot for the available MSWI samples, produced at the Institute for Rock Magnetism of the University of Minnesota, is reported in Figure S2. The reader can also refer to the data repository of the Institute for Rock Magnetism and rock magnetic bestiaries using Rock Mag software available at <http://www.irm.umn.edu/>. Other magnetic data (e.g.,  $\kappa_{fd}\%$ ,  $\chi$ ,  $S_{-0.3T}$ ,  $MDF_{ARM}$ ,  $B_{0cr}$ ) and its descriptive statistics are reported in the companion article [1].

### S2. DATA on (geo)chemical composition of the sample materials

Table S2 reports the XRF measures on thin-layer pressed powder pellets of the sample materials (after Loss on Ignition, LOI, correction). Major elements are expressed as their oxides.

### S3. DATA on morphology and mineralogy of the sample materials

Figure S3 and Figure S4 are scanning electron microscope (SEM) observation of representative samples of BA and FA. Microphotographs on the right refer to BA at a different scale of magnification (of the same specimen), while the FA sample is on the left.

Figures S5 and S6 show elemental maps of concentration of representative samples for selected elements using Energy-dispersive X-ray spectroscopy (EDS) coupled to the SEM. Figures S5 and S6 supplement Figure 6 of [1].

### S4. Statistical DATA analysis

Here the statistical data analysis is reported in the supplementary materials as it was described and used to support discussion in [1]. Table S3 and S4 report the Pearson Correlation

Table S2

Major and trace element composition of BA and FA samples collected in four MSWI plants of Northern Italy. FA suffixed with U = untreated collected after the combustion chamber, L = treated in bag filters using lime additive, S = treated in bag filters using soda additive, E = collected via electrostatic precipitators.

		MSWI	SiO <sub>2</sub>	TiO <sub>2</sub>	AlO <sub>3</sub>	Fe <sub>2</sub> O <sub>3</sub>	MgO	CaO	MnO	K <sub>2</sub> O	P <sub>2</sub> O <sub>5</sub>	Cu	Cr	Ce	Co	Ga	La	Mo	Nb	Nd	Ni	Pb	V	Zn	Zr	
sample	unit	n°	g/100g	g/100g	g/100g	g/100g	g/100g	g/100g	g/100g	g/100g	g/100g	mg/kg	mg/kg	mg/kg	mg/kg	mg/kg	mg/kg	mg/kg	mg/kg	mg/kg	mg/kg	mg/kg	mg/kg	mg/kg	mg/kg	
BA1.1	1	1	39.2	1.4	11.0	10.0	2.7	17.8	0.1	1.4	2.3	2810	637	34	32	11	19	21	18	12	202	927	105	2644	87	
BA1.2		1	36.7	1.0	10.2	9.4	3.0	19.2	0.1	1.2	2.3	5535	557	32	24	11	18	22	15	12	246	3881	363	2132	491	
BA1.3		1	37.0	1.1	10.2	9.5	3.1	19.9	0.1	1.4	2.5	4379	630	34	31	11	20	21	15	15	276	2474	385	2632	279	
BA1.4		1	37.3	1.2	10.2	9.6	3.1	20.7	0.1	1.5	2.8	3222	703	36	39	11	23	21	14	18	306	1066	407	3132	68	
BA1.5		1	36.7	1.3	10.3	10.0	2.7	17.6	0.1	1.3	2.1	3844	613	34	23	10	18	20	16	12	196	1848	174	2194	226	
BA1.6		1	35.6	1.3	10.4	10.1	2.6	17.5	0.1	1.3	2.2	3392	627	33	31	10	18	20	17	12	205	1028	106	2700	92	
BA1.7		1	33.0	1.1	10.0	10.0	2.7	18.9	0.1	1.3	2.4	3986	636	33	38	10	19	20	15	14	263	1238	226	3198	87	
BA2.1		2	1	27.6	1.0	8.4	7.6	1.9	21.6	0.1	1.0	1.2	2768	671	31	30	8	16	10	9	14	127	1260	23	2788	65
BA2.2	1		29.3	1.2	9.3	6.9	2.0	26.0	0.1	1.1	1.5	3904	910	28	23	9	14	15	9	12	233	1645	27	3610	81	
BA2.3	1		28.2	1.1	8.7	7.4	2.0	23.0	0.1	1.1	1.3	3147	751	30	28	8	16	12	9	13	162	1389	24	3062	71	
BA2.4	1		27.6	1.1	8.1	7.2	2.0	22.0	0.1	1.0	1.3	2536	770	32	32	8	18	9	9	15	117	1080	23	3356	68	
BA2.5	1		31.5	1.0	9.5	9.2	2.6	18.0	0.1	1.2	2.3	3766	574	32	46	10	20	20	13	13	242	1147	244	3374	57	
BA2.6	1		28.4	1.1	8.7	7.1	2.0	24.0	0.1	1.1	1.4	3220	840	30	27	8	16	12	9	13	175	1363	25	3483	75	
BA2.7	1		28.5	1.1	9.0	7.4	2.0	23.6	0.1	1.1	1.4	3453	741	29	26	9	14	13	9	13	185	1543	25	2915	72	
BA2.8	1		27.6	1.0	8.4	7.6	1.9	21.6	0.1	1.0	1.2	2768	671	31	30	8	16	10	9	14	127	1260	23	2788	65	
BA3.1	3	1	25.2	1.1	4.8	7.8	2.3	33.8	0.1	0.7	0.8	1567	508	16	18	5	29	11	16	13	72	293	26	2081	130	
BA3.2		1	25.2	1.1	4.8	7.8	2.3	33.8	0.1	0.7	0.8	1567	508	16	18	5	29	11	16	13	72	293	26	2061	130	
BA3.3		1	25.2	1.1	4.8	7.8	2.3	33.8	0.1	0.7	0.8	1567	508	16	18	5	29	11	16	13	72	293	26	2054	130	
BA3.4		1	35.5	0.6	4.3	8.2	2.1	24.9	0.1	0.6	0.7	648	1002	21	14	4	26	8	15	15	55	173	21	1625	115	
BA3.5		1	22.8	1.3	5.4	8.0	2.4	34.6	0.1	0.7	1.0	1836	278	15	20	6	38	12	18	15	73	320	30	2182	133	
BA3.6		1	17.2	1.3	4.6	7.3	2.2	41.8	0.1	0.6	0.9	2216	244	11	19	5	22	12	16	9	89	385	28	2373	141	
BA4.1		4	1	29.5	0.9	6.5	6.1	3.4	28.6	0.1	0.9	1.2	1376	309	16	19	8	5	8	6	6	70	610	28	1839	220
BA4.2			1	29.5	0.9	6.5	6.1	3.4	28.6	0.1	0.9	1.2	1376	309	16	19	8	5	8	6	6	70	610	28	1833	220
BA4.3	1		29.5	0.9	6.5	6.1	3.4	28.6	0.1	0.9	1.2	1376	309	16	19	8	5	8	6	6	70	610	28	1833	220	
BA4.4	1		36.9	0.5	5.1	6.4	3.2	24.3	0.1	0.9	0.9	863	275	19	15	7	3	6	4	6	62	1146	23	1073	172	
BA4.5	1		30.3	0.9	7.4	7.1	3.9	25.9	0.2	1.1	1.3	1526	329	13	22	8	9	8	7	5	68	370	31	2176	262	
BA4.6	1		21.1	1.1	6.8	4.8	2.9	35.8	0.1	0.8	1.4	1740	324	17	20	8	4	9	7	7	81	315	29	2251	225	
Bottom ashes average	1		30.1	1.1	7.8	7.9	2.6	25.4	0.1	1.0	1.5	2607	564	25	25	8	17	13	12	12	145	1058	93	2496	147	
FAU1.1	1		1	13.9	1.3	5.2	2.3	5.4	24.9	0.1	5.1	1.5	910	941	21	21	8	12	18	11	8	76	3586	20	11998	66
FAU1.2		1	13.9	1.3	5.2	2.3	5.4	24.9	0.1	5.1	1.5	910	941	21	21	8	12	18	11	8	76	3586	20	11991	66	
FAS1.1		1	1.4	0.1	0.3	0.2	0.6	1.9	0.1	9.1	1.3	1286	590	19	23	11	10	45	22	6	292	5066	12	24739	67	
FAS1.2		1	1.4	0.1	0.3	0.2	0.6	1.9	0.1	9.1	1.3	1286	590	19	23	11	10	45	22	6	292	5066	12	24281	67	
FAU2.1		2	1	14.0	1.5	6.0	1.7	1.9	27.0	0.0	2.3	0.1	670	53	2	2	3	1	10	1	1	18	2585	0	9817	22
FAU2.2			1	14.0	1.5	6.0	1.7	1.9	27.0	0.0	2.3	0.1	670	53	2	2	3	1	10	1	1	18	2585	0	9756	22
FAL3.1		3	1	5.1	0.6	2.3	1.0	1.0	30.5	0.1	4.3	1.4	993	328	19	21	8	12	23	10	6	95	2388	17	14837	76
FAL3.2			1	5.1	0.6	2.3	1.0	1.0	30.5	0.1	4.3	1.4	993	328	19	21	8	12	23	10	6	95	2388	17	14834	76
FAU3.1	1		16.3	1.7	7.3	1.9	2.1	29.9	0.0	3.2	0.6	824	238	11	9	4	8	37	4	6	56	2982	31	8202	46	
FAU3.2	1		16.3	1.7	7.3	1.9	2.1	29.9	0.0	3.2	0.6	824	238	11	9	4	8	37	4	6	56	2982	31	8193	46	
FAE4.1	4	1	14.0	1.2	5.2	2.0	1.4	18.5	0.1	2.2	1.7	499	989	26	17	7	14	22	13	10	81	573	26	4305	54	
FAE4.1		1	14.0	1.2	5.2	2.0	1.4	18.5	0.1	2.2	1.7	499	989	26	17	7	14	22	13	10	81	573	26	4341	54	
Fly ashes average			10.8	1.1	4.4	1.5	2.1	22.1	0.0	4.4	1.1	864	523	16	16	7	9	26	10	6	103	2863	18	12274	55	

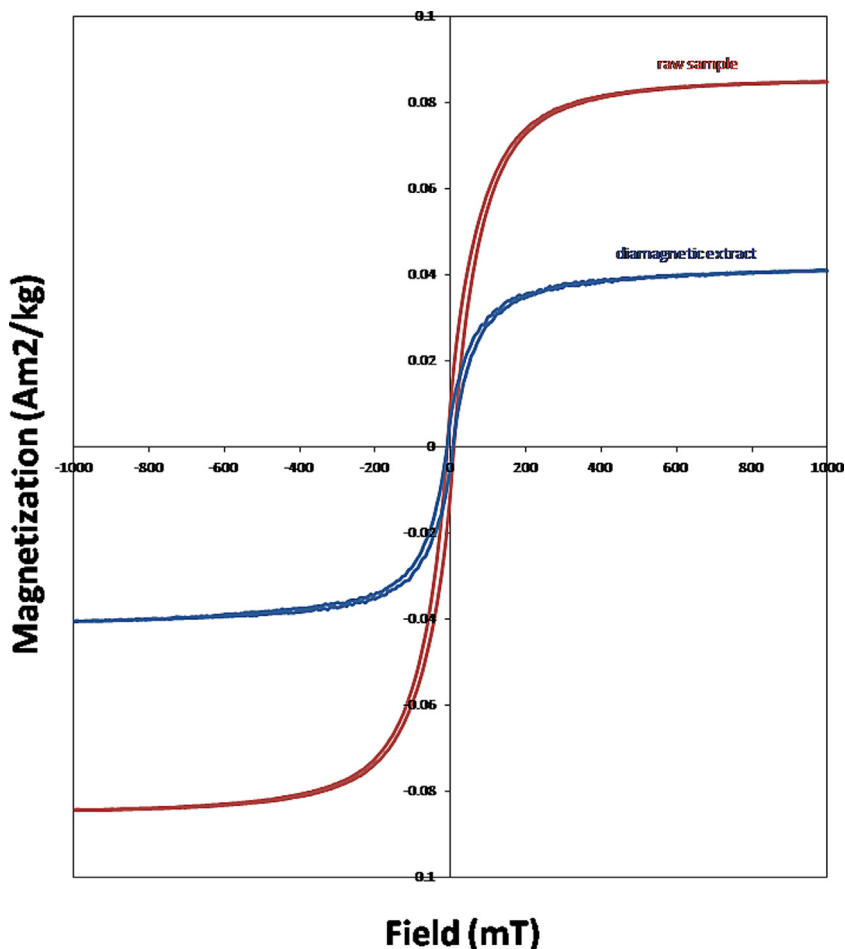


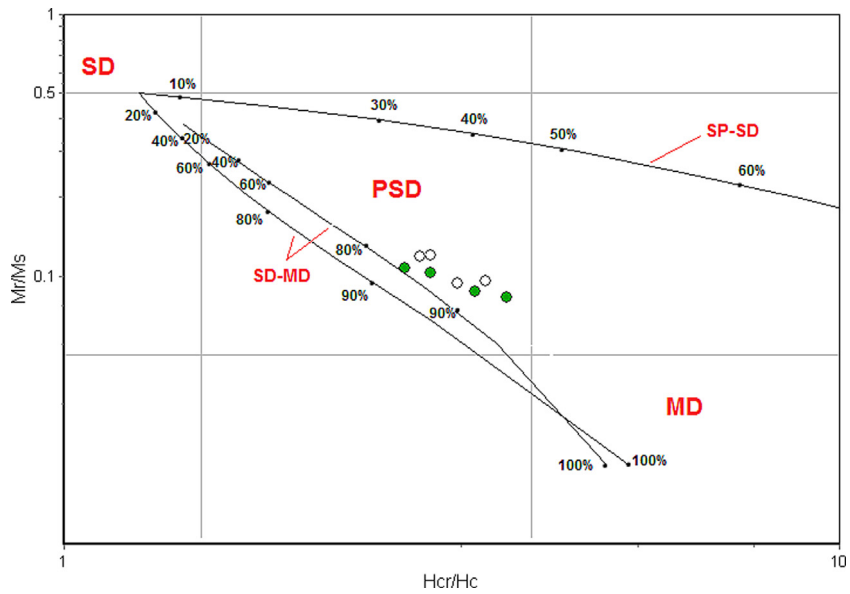
**Fig. S1.** Hysteresis loops for MSWI BA and its “more diamagnetic” extract after magnetic separation.

Analysis (filtered: applied to different groups of observations). Table S3 relates selected XRF measurands vs magnetic parameters  $\kappa_{fd}\%$ ,  $\chi$ ,  $S_{-0.3T}$ , and  $B_{0cr}$ . Table S4 shows the correlation of the geochemical data for BA, FA, and BA+FA. Figure S8 reports Principal Component Analysis (PCA). Figure S9 and Figure S10 report different Cluster Analysis (filtered: cluster variables vs cluster observation). Figure S11 reports different probability plots (PP) based on selected magnetic parameters, i.e.,  $SIRM/\chi$  (S11-PP1),  $B_{0cr}$  (S11-PP2), and  $MDF_{ARM}$  (S11-PP3).

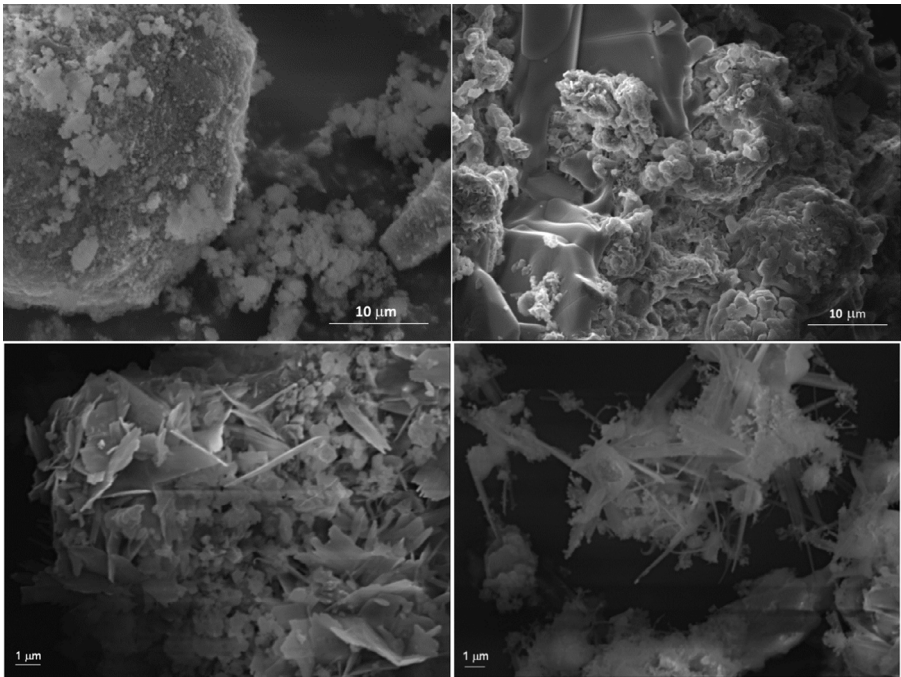
#### S5. Comparison of magnetic and geochemical DATA using biplots

Figure S12 is a SIRM vs  $\kappa_{ARM}$  plot showing information about MSWI plants.

A further application of several biplots of magnetic vs geochemical data is reported in the supplementary materials (Figure S13 composed of 4 panels; Figure S14 of 26 panels) as it needs to be evaluated all together, also with the support of the discussion section from the companion article [1]. Figure S13 displays other biplots of magnetic parameters (with geochemical and sample information displayed). Figure S14 refers to different panels showing biplots of magnetic parameters with contouring of elemental concentrations for selected XRF measurands. For S14-



**Fig. S2.** The Day Plot of available MSWI residues (BA solid circles; FA empty circles). Reference lines for magnetic state domains are also displayed.



**Fig. S3.** SEM observation of MSWI BA and FA (coated stub).

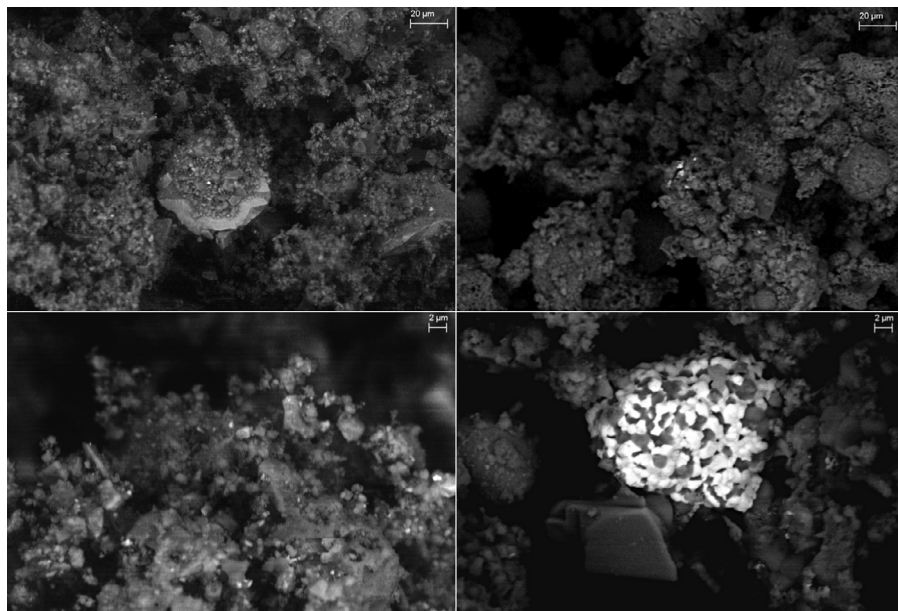


**Fig. S4.** SEM observation of MSWI BA and FA (uncoated stub).

1 panels, contouring is based on the entire data set, while S14-2 panels exemplify contouring using BA and FA samples as separated data set. These basic magnetic plots complemented with geographic or chemical information can serve to distinguish the provenance of MSWI residues as well as allow quick identification of magnetic mineralogies and potential metal enrichments, respectively.

## 2. Experimental Design, Materials, and Methods

The measured magnetic parameters rely on fundamental environmental magnetic studies such as [3,4,8–12]. The methods used for statistical data analysis can be found in [7].

### 2.1. Collection of MSWI samples

The collection of BA and FA samples derived from four Italian MSWI systems [1] is considered in the present work. The sampling methodology can be found elsewhere [2]. The selected facilities are located in four municipalities of northern Italy and serve an area of about 10000 km<sup>2</sup> within the Po Valley, one of the most densely populated areas of the Country. Each incinerator is equipped with a grate-furnace system and operates at temperatures as high as 850–1100°C. Further information is available elsewhere [12, 13]. The solid waste input averages  $1.5 \cdot 10^5$  tons per annum, consisting of 90% household waste and 10% special waste. The fraction of special waste includes scraps from ceramics, processing waste from steel-making industries, car fluff (also referred to as automobile shredder residues, ASR), and hospital and pharmaceutical waste in minor proportion. The solid waste output averages  $4.6 \cdot 10^4$  t/a and  $4.1 \cdot 10^3$  t/a for BA and FA, respectively. The figure for BA does not include the ferrous metal scraps (ranging 5–8  $\cdot 10^3$  t/a) that are recovered by a rough magnetic separation after quenching and re-melted for reuse generally by a third party company. The ferrous metal fraction is, therefore, not considered here. The available FA samples accounted for different categories depending on the technology of the air



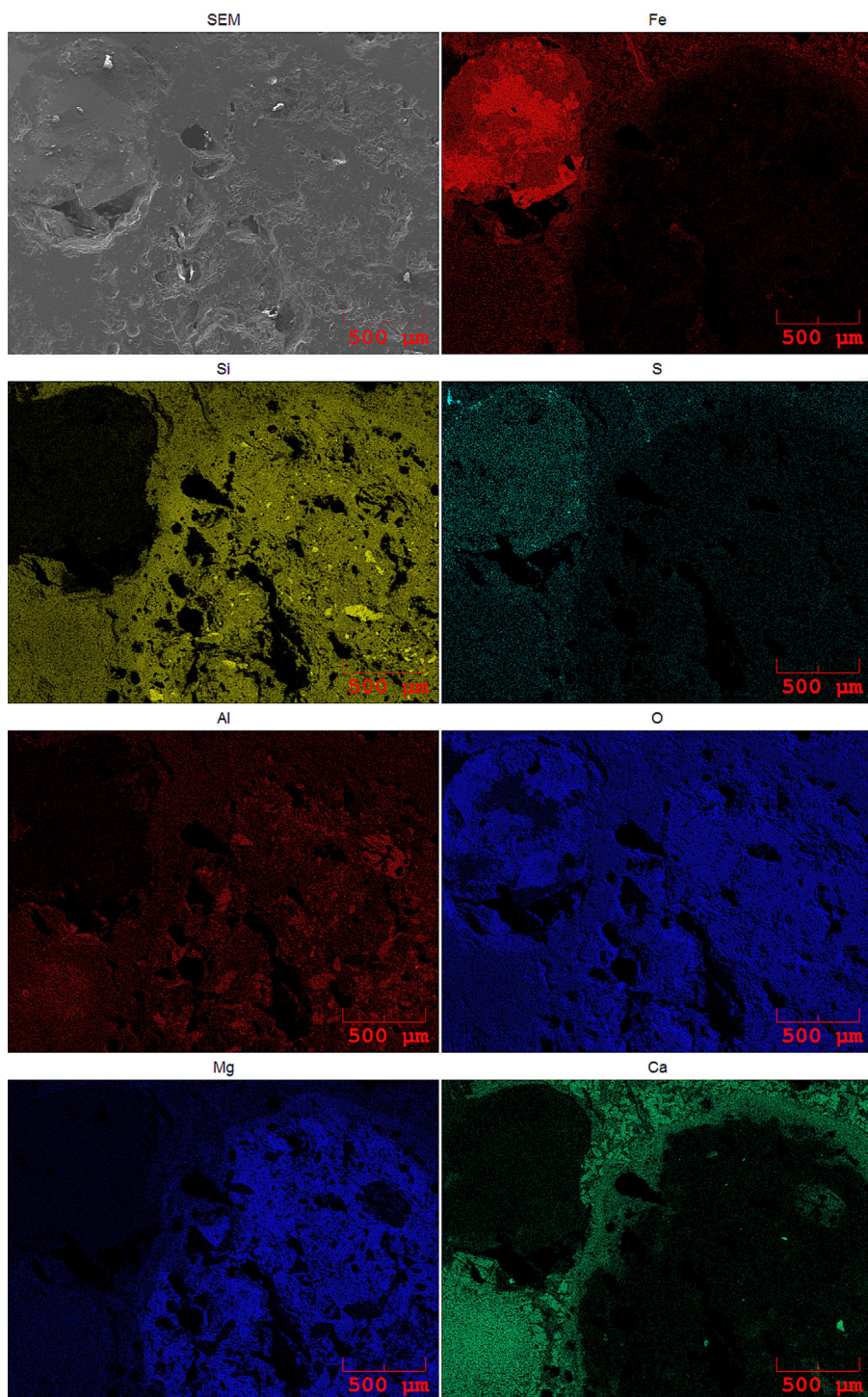


**Fig. S5.** Elemental maps of concentration of MSWI BA (coated thin section).



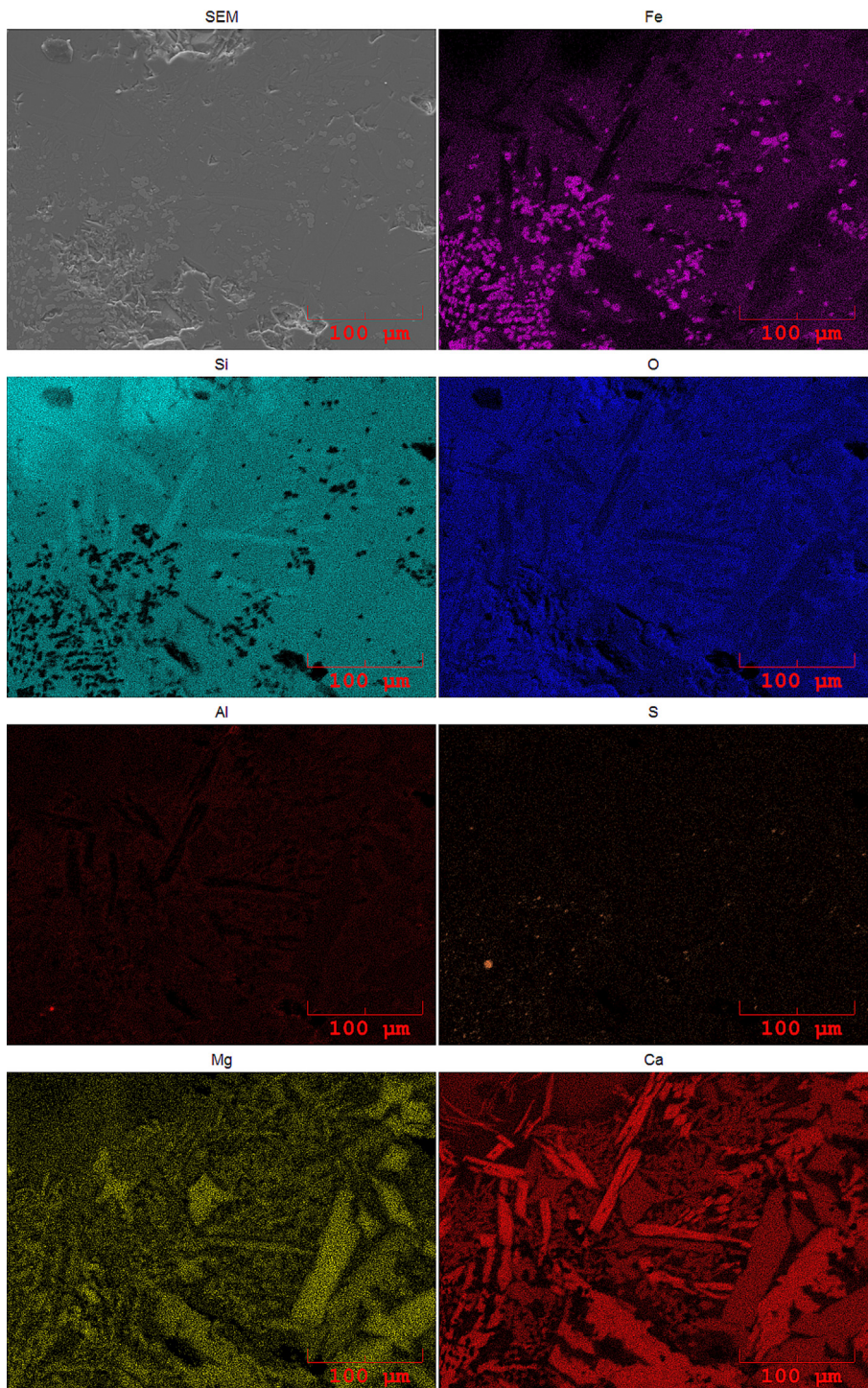


**Fig. S6.** Elemental maps of concentration of MSWI FA magnetic extract (coated thin section).

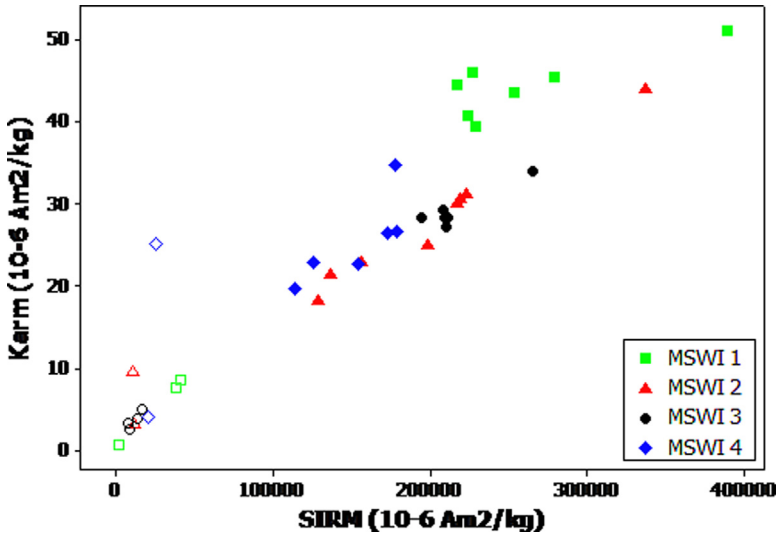


**Fig. S12.** SIRM vs  $K_{ARM}$  plot for the dataset of BA (solid symbols) and FA (empty symbols). Colours refer to the four MSWI plants.

pollution control system [12]. Four types of FA were collected in the selected MSWI plants when possible, namely: at the first step after the combustion chamber (FAU, ascribed as untreated), the electrostatic precipitator (FAE) and the FA recovered via bag filters chemically treated using soda (FAS) and lime (FAL) as standard cleaning up options. We assumed that each sample is representative of the MSWI ash category of each MSWI plant and refer to the sampling made during 2013. The variability of a given plant over time cannot be considered, thereby spatiotemporal variations of MSWI ashes are not assessed in this work. The present dataset further discussed in [1] can serve as an averaged reference for the north Italian region and as a ground basis for intercomparison. Furthermore, these samples are assumed to be a reliable reference for MSWI plants that represent one fourth of waste processing capacity of a country since they burn more than 25% total waste of the region.

The sample-set is composed of 47 samples, including eight magnetic extracts of selected BA and FA materials. The analysis of magnetic extracts allowed to characterize better a weakly magnetic fraction and a more magnetic one of the same specimen, referred to as “more diamagnetic extract” and “magnetic extract”, respectively, in agreement to [1].

## 2.2. Samples pre-treatment

The material pre-treatment included 1) drying at 40°C for one week; 2) hand-sorting and removal of the most significant metallic fragments, e.g., partly melted screws, bolts and cans, found in the BA samples; 3) homogenization with an agate rotating mill disk. Magnetic and more diamagnetic extracts were separated using a Frantz magnetic separator by imparting a 1.1 A current in the laminar isodynamic region and a +15° side slope of the chute [13]. This latter pre-treatment is referred to as magnetic separation in [1].

## 2.3. Magnetic measurements

An assortment of magnetic measurements was performed on triplicate samples at the Institute of Marine Sciences of the National Research Centre (ISMAR-CNR, Bologna Research Area).

Magnetic susceptibility at room temperature was measured at two different frequencies (0.47 and 4.7 kHz) by using a dual-frequency MS2B Bartington meter (Bartington Instruments Ltd, UK). The difference between the two measured values allowed to calculate the frequency dependence of susceptibility ( $\kappa_{fd}\%$ ). A magnetic reference material, i.e., a permalloy standard, was used for the calibration of the Bartington meter. Samples of dried powder were laid down and gently compacted in cubic plastic boxes of a standard volume of 8 cm<sup>3</sup>. Mass specific magnetic susceptibility ( $\chi$ ) was calculated by dividing the volume susceptibility ( $\kappa$ ), previously corrected for the drift, over the sample mass annotated for each sample. An induced anhysteretic remanent magnetization (ARM) was imparted by an AGICO LDA-3A AF demagnetizer to all samples using a peak alternating field (AF) of 100 mT with a biasing superimposed direct current (DC) field of 0.1 mT parallel to the AF; the mass-specific susceptibility of ARM ( $\chi_{ARM}$ ), expressed in m<sup>3</sup>/kg, was calculated after mass-normalization and bias DC field correction. Isothermal remanent magnetization (IRM) experiments were conducted on a pulse magnetizer (ASC IM-30). An IRM up to 1.0 T was imparted, followed by a reverse field of IRM in five steps up to 0.4 T. The IRM acquired in a field of 1.0 T was regarded as the saturation IRM (SIRM). From the measured value, expressed in A/m, the mass magnetization is calculated by dividing for volume and mass weight of the sample in Am<sup>2</sup>/kg. The IRM experiments allowed the calculation of additional parameters such as the coercivity of remanence (B<sub>0cr</sub>) and the S-ratio. The S-ratio is defined as IRM-300mT/SIRM, where IRM-300mT is the backfield IRM at a field of 300 mT. As a consequence, it can also be denoted as S<sub>-0.3T</sub>. Hysteresis loops and backfield curves at room temperature were previously measured on selected samples at the Institute for Rock Magnetism (IRM, University of Minnesota), using a MicroMag Princeton Measurements Vibrating Sample Magnetometer (VSM) capable of a nominal sensitivity of 5•10<sup>-9</sup> Am<sup>2</sup>. Hysteresis properties of selected samples of MSWI ashes are also available at <http://www.irm.umn.edu/> and referred as to Italian MSWI (further inquiry to obtain the raw data can be made to the IRM, after authorization from the corresponding author).

## 2.4. Geochemical and mineralogical analysis

The analysis of the chemical and mineralogical composition of the sample material was performed at the Department BiGeA (University of Bologna) and the Department of Physics and Earth Sciences (University of Parma) as complementary information to magnetic data. Particles morphology and dimensions were assessed at different magnification on a Scanning Electron Microscope (SEM), JEOL JSM-6480LV high-performance, capable of working at variable pressure with secondary electron and backscattered electron imaging detectors. BA and FA samples were prepared on stubs and thin section coated with gold or uncoated. Selected samples are imaged with a SEM ZEISS LEO 1530 FEG without metallization at the Institute for Microelectronics and Microsystems (IMM-CNR, Bologna Research Area). The bulk chemical composition was determined by X-ray fluorescence (XRF) using a wavelength-dispersive spectrometer (WD-XRF), PAN-Alytical, Axios 4000. The sample preparation for XRF analysis relied on pressed powder pellet ( $\phi$ 37 mm) in a boric acid binder, using three grams of the dried and milled sample. The estimated precision for major and trace element determinations are better than 5% except for measurands whose detected concentrations were as low as 10 mg/kg (10–15%). After correction for the Loss on Ignition (LOI), several analytes were measured by XRF: Si, Ti, Al, Fe, Mn, Ca, Cu, Ni, Mo, Pb, Zn, Zr, and those metals considered as “critical” in [2], such as Mg, Cr, Co, Ga, Nb, V, and the light rare earth elements (LREE) La, Ce, and Nd.

## 2.5. Statistical data analysis

We used multivariate statistics to evaluate the available data. Pearson's correlation coefficient analysis (PC), principal component analysis (PCA), and cluster analysis (CA) helped to examine

the relations between the geochemical and magnetic data. In particular, The CA using Ward's linkage and Euclidean distances are performed as cluster observations and cluster variables [7]. The PC analysis helped to define the correlation between the measured chemical concentrations and other magnetic or chemical parameters. The PCA incorporated magnetic and geochemical data after standardization and provided with a unified comparison which, in turn, allowed to use optimized minimum factors to explain the original data set. The statistical analyses and observations referred to the entire dataset except for magnetic extracts serving to avoid any dependence between variables and observations. The outcomes from the PCA, cluster observations and cluster variables evaluated and further confirmed the similarities between the variables.

## Declaration of Competing Interest

The authors declare that the research was conducted in the absence of any commercial or financial relationships that could be construed as a potential conflict of interest.

## Acknowledgments

Part of this work was performed at the laboratory of Paleomagnetism of the ISMAR-CNR; Institute for Rock Magnetism (IRM), University of Minnesota, thanks to an IRM Visiting Fellowship to V.F.; at the BiGeA Department under the project SuoliBO-HD funded by the Fondazione Carisbo to V.F. and E.D.; at the IMM-CNR (Bologna Research Area) thanks to the assistance of Franco Corticelli, Lucilla Capotondi, and Marzia Rovere. We acknowledge the financial support from project PRIN 2017 - 2017L83S77 (MINERAL REACTIVITY, A KEY TO UNDERSTAND LARGE-SCALE PROCESSES: FROM ROCK FORMING ENVIRONMENTS TO SOLID WASTE RECOVERING/LITHIFICATION).

## Associated research article

Funari, V., Mantovani, L., Vigliotti, L., Dinelli, E., & Tribaudino, M. (2020). *Understanding room-temperature magnetic properties of anthropogenic ashes from municipal solid waste incineration to assess potential impacts and resources*. Journal of Cleaner Production, 262, 121209. <https://doi.org/10.1016/j.jclepro.2020.121209>

## Supplementary materials

Supplementary material associated with this article can be found, in the online version, at [doi:10.1016/j.dib.2020.105728](https://doi.org/10.1016/j.dib.2020.105728).

## References

- [1] V. Funari, L. Mantovani, L. Vigliotti, E. Dinelli, M. Tribaudino, Understanding room-temperature magnetic properties of anthropogenic ashes from municipal solid waste incineration to assess potential impacts and resources, J. Clean. Prod. 262 (2020) 121209 [doi.org/10.1016/j.jclepro.2020.121209](https://doi.org/10.1016/j.jclepro.2020.121209).
- [2] V. Funari, R. Braga, S.N.H. Bokhari, E. Dinelli, T. Meisel, Solid residues from Italian municipal solid waste incinerators: A source for "critical" raw materials, Waste Manag 45 (2015) 206–216.
- [3] B.A. Maher, Magnetic properties of some synthetic sub-micron magnetites, Geophys. J. 94 (1988) 83–96.
- [4] R. Thompson, F. Oldfield, Environmental Magnetism, 1st ed., Springer, London/Netherlands, 1986.
- [5] Q. Liu, et al., Environmental magnetism: Principles and applications, Rev. Geophys. 50 (2012).
- [6] V. Funari, Magnetic characterization of solid by-products from Municipal Solid Waste Incinerators, IRM Q 26 (2016) 2–3.
- [7] C. Reimann, P. Filzmoser, R. Garrett, R. Dutter, Statistical Data Analysis Explained - Applied Environmental Statistics with R, © 2008 Joh. Wiley, 2008.

- [8] F. Oldfield, Environmental magnetism - A personal perspective, *Quat. Sci. Rev.* 10 (1) (1991) 73–85.
- [9] C.P. Hunt, et al., Rock-magnetic proxies of climate change in the loess-palaeosol sequences of the western Loess Plateau of China, *Geophys. J. Int.* 123 (1995) 232–244.
- [10] B. M. Moskowitz, M. Jackson, and V. Chandler, “Geophysical Properties of the Near-Surface Earth: Magnetic Properties” pp. 139–174, 2015.
- [11] D.J. Dunlop, Theory and application of the Day plot ( $M_s/M_s$  versus  $H_{cr}/H_c$ ) 1. Theoretical curves and tests using titanomagnetite data, *J. Geophys. Res.* 107 (B3) (2002) 2056.
- [12] V. Funari, S.N.H. Bokhari, L. Vigliotti, T. Meisel, R. Braga, The rare earth elements in municipal solid waste incinerators ash and promising tools for their prospecting, *J. Hazard. Mater.* 301 (Jan. 2016) 471–479.
- [13] V. Funari, L. Mantovani, L. Vigliotti, M. Tribaudino, E. Dinelli, R. Braga, Superparamagnetic iron oxides nanoparticles from municipal solid waste incinerators, *Sci. Total Environ.* 621 (2018) 687–696.